POAC'11
Montréal, Canada

Proceedings of the 21st International Conference on
Port and Ocean Engineering under Arctic Conditions
July 10-14, 2011
Montréal, Canada

POAC11-033

Three Dimensionless Independent Parameters to Fully Describe and Estimate Dimensionless Ice-Induced Pressures on Vertical Structures

Aaruun V. M. Arunachalam
College of the North Atlantic, Burin Campus
Burin-Bay Arm, Newfoundland, Canada

ABSTRACT

Following Leggett and Gold dimensional variables defining ice-induced pressures on vertical structures (B, h, u, E, σ_f, K_{IC}, ρ_i, g) were identified. Applying dimensional analysis, following Atkins, these dimensional variables were reduced to dimensionless dependent variable ($p_e/\rho_i u^2$) and a limited number of dimensionless independent parameters, namely aspect ratio (B/h), dimensionless velocity [$u/\sqrt{(gh)}$] and dimensionless material properties. A large number of experimental data from physical model tests and field tests, using different types of ice - freshwater ice, seawater ice, and model ice were analyzed, following rigorous requirements of dimensional analysis. (1) It was found that when other conditions remain same, dimensionless ice-induced pressure ($p_e/\rho_i u^2$) on rigid vertical structures decreases with (a) increasing aspect ratio (B/h), at a rate of about 0.42; (b) increasing dimensionless velocity or dimensionless strain-rate or thickness Froude number [$u/\sqrt{(gh)}$] at a rate of about 1.80 when $u/\sqrt{(gh)}$ is < about $6.0\times10^{-3}$and at a rate of about 1.93 when $u/\sqrt{(gh)}$ is > about 6.0×10^{-3}. (2) It was also found that shapes of structures do not influence dimensionless ice-induced pressures on structures. (3) Qualitative influence of material properties of ice has been identified, which shows that when other conditions, namely (B/h), and [$u/\sqrt{(gh)}$], remain same, ($p_e/\rho_i u^2$) for sea-ice interaction is about 1.8 orders of magnitude less than that for freshwater ice interaction. Analyses to establish the exact influence of dimensionless material properties on dimensional ice-induced pressure quantitatively is in progress, completion of which will lead to development of an empirical relationship for dimensional ice-induced pressure on vertical structure.

INTRODUCTION

In the preface of proceedings of the conference on "Ice pressures against structures", held in Laval University in 1966, Crawford (1966), then Chair of the Associate Committee on Geotechnical Research noted "Although the problem (*of the force exerted by sheet-ice on structures*) has been with us for many years, there is still not available to engineers the information required to predict these forces with a satisfactory degree of confidence". In the last 45 years since this observation was made, a large number of experimental data have been generated through laboratory model tests and field tests, using different types of ice (freshwater

ice, sea ice, model ice of different types). Analytical and numerical models (FEM, DEM, BEM etc) have been attempted. In spite of all these developments, the ability of engineers to accurately predict ice-induced forces on structures due to an interaction event remains uncertain, even today, as was noted by Crawford 45 years ago.

Uncertainty in Prediction of ice-induced Pressures, PA Diagram, Size Effect, Fracture Mechanics

The ability of engineers to predict ice-induced pressures on structures due to an interaction event, either accurately or with a satisfactory level of confidence, can be understood from the outcome of various surveys conducted by Sanderson (1986), Croasdale and Kennedy (1996), Croasdale and Brown (2000), Schwarz (2001), Timco (2006) which show that there is a difference of about one order of magnitude between the lowest and the highest value predicted for a given interaction scenario, even among experts involved. This uncertainty can partly be attributed to some extent on the arrival of Pressure-Area Diagram of Sanderson (1986), which contains data representing several types of ice, and a range of temperatures, salinities and strain-rates (Ghoneim et al, 2010). The influence of material properties, strain-rates, however, has not been separated out from the PA diagram. Based on Sanderson's PA diagram, modified PA diagram of Masterson et al (2006) and Palmer et al (2009) have been presented. From such PA diagrams, it is suggested that the observed decrease of pressure with increasing contact area is due to fracture behavior of ice.

In studying the size effect on the material property (σ_N) of concrete and rock, due to known applied static load, Bazant (1984) notes, "To separate the size effect (*on material properties*) from other influences one must consider structures of different sizes but geometrically similar shapes (e.g., beams of same span-to-depth ratio and same crack length-to-depth ratio)". This implies that before we embark on exploring size effect in ice-induced pressure, we should attempt to separate out any influences due to other parameters, aspect ratio (B/h), dimensionless velocity [$u/\sqrt{(gh)}$] and dimensionless material properties.

Before PA Diagram of Sanderson came into the collective conscience of researchers in ice-engineering, it was known and accepted at least qualitatively, that ice-induced pressures on structures depends on:

- Aspect ratio (B/h) effect (Afanasev et al, 1971; Korzhavin, 1971; Frederking and Gold, 1975; Neill, 1976; Lipsett and Gerard, 1975; Kato and Sodhi, 1983; Timco, 1986; Cammaert and Muggeridge, 1988) and others.
- Strain-rate (u/h or u/B) or velocity effect (Michel, 1970; Michel and Toussaint, 1977; Ralston, 1979; Nadreau and Michel, 1982; Cammaert and Muggeridge, 1988), and others
- Material properties (E, σ_f, K_{IC}) of ice (Cammaert and Muggeridge, 1988; Zufelt and Ettema, 1996) and others.

After Pressure-Area Diagram was introduced in ice-engineering literature, influence of aspect ratio, strain-rate (velocity), and material properties of ice on ice-induced pressures on structures appears to have been neglected. This paper aims to quantitatively establish the influence of the three parameters – aspect ratio (B/h), strain-rate (u/h) and material properties (E, σ_f, K_{IC}) of ice - on ice-induced pressures on rigid vertical structures - through dimensional analysis and similarity theory approach, in conjunction with analyses of a large number of experimental data.

DEFING ICE-STRUCTURE INTERACTION PROBLEM

Following Leggett and Gold (1966), ice-induced pressure (p_e) on vertical structures can be given in terms influencing dimensional parameters as:

$$p_e = \phi_1 \left\{ B,\ h,\ u,\ E,\ \sigma_f,\ K_{IC},\ \rho_i,\ g \right\} \qquad (1)$$

where, B = width of structure; h = ice thickness; u = ice velocity; E = modulus of elasticity; σ_f = bending strength; K_{IC} = fracture toughness; and ρ_i = density of sheet ice, and g = acceleration due to gravity.

Dimensionless form of representing dependent variable and independent parameters

Dimensionless form of representation (as mere numbers) of dependent variable and independent parameters to complex problems involving many variables – such as ice-structure interaction problems - would help understand properly the physics of the problem being studied (Langaar, 1951; Pankhurst, 1960; Taylor, 1974; Sharp, 1981; Barenblatt, 1987). It is the aim of this paper to represent dependent variable and independent parameters defining ice-structure interaction problem in dimensionless form and analyze available experimental results in strict accordance with the requirements of dimensional analysis and similarity theory and see if we can improve our ability to accurately predict ice-induced pressures on vertical structures to an acceptable level.

Dimensionless variables for ice-structure interaction problem

Through application of dimensional analysis and similarity theory to the complex ice-structure interaction problem following Atkins (1975; 1985), the dimensionless form of ice-induced pressures ($p_e/\rho_i u^2$) on a rigid vertical structures can be expressed for purely ductile deformation (Eqn. 2) and for combined ductile and fracture deformation (Eqn. 3) of ice in terms of dimensionless independent parameters as:

$$\left(\frac{p_e}{\rho u^2}\right) = \phi_2 \left\{ \left(\frac{B}{h}\right), \left(\frac{u}{\sqrt{g\,h}}\right), \left(\frac{E}{\sigma_f}\right), \left(\frac{\rho u^2}{E}\right) \right\} \qquad (2)$$

$$\left(\frac{p_e}{\rho u^2}\right) = \phi_3 \left\{ \left(\frac{B}{h}\right), \left(\frac{u}{\sqrt{g\,h}}\right), \left(\frac{\sigma_f \sqrt{h}}{K_{IC}}\right), \left(\frac{\rho u^2 \sqrt{h}}{K_{IC}}\right), \left(\frac{E}{\sigma_f}\right) \right\} \qquad (3)$$

where, B/h = aspect ratio; $u/\sqrt{(gh)}$ = dimensionless velocity or dimensionless strain-rate or thickness Froude number (*TFN*); and (E/σ_f), $(\sigma_f\sqrt{h}/K_{Ic})$, $(\rho_i u^2\sqrt{h}/K_{Ic})$, are dimensionless material parameters of ice.

ANALYSIS OF EXPERIMENTAL DATA IN DIMENSIONLESS FORM OF PARAMETERS

We analyzed a large number of experimental data that were included in the generation of PA diagram of Sanderson as well as those data published after the PA diagram, in the context of Eqns. 2 and 3. Some of the results are presented and briefly discussed in the following pages. The values of primary and derived experimental parameters used in the current analyses shown in Figures 1 to 5 are shown in Table 1.

Table 1: Primary and derived experimental parameters of interest from various datasets used in the present analysis.

Reference	Lab /Field	FWI /SWI	B (m)	h (m)	u (m/s)	u/h (s^{-1})	u/B (s^{-1})	TFN $u/\sqrt{(gh)}$	Asp Rat (B/h)	E (Pa)	σ_f (Pa)	Pres (Pa)
Hirayama (1974)	Lab	FWI	6.0×10^{-3} to 1.5×10^{-1}	6.0×10^{-3} to 6.0×10^{-2}	4.0×10^{-5} to 1.5×10^{-2}	1.0×10^{-3} to 1.8×10^{0}	1.0×10^{-3} to 5.0×10^{-1}	7.3×10^{-5} to 1.1×10^{-2}	3.0×10^{-1} to 4.2×10^{0}		3.5×10^{6} (Comp)	
Finn (1971)	Lab	FWI	8.0×10^{-2} to 1.2×10^{-1}	2.6×10^{-2} to 4.6×10^{-2}	2.0×10^{-4} to 4.0×10^{-1}	4.1×10^{-3} to 5.6×10^{0}	1.6×10^{-3} to 5.1×10^{0}	2.9×10^{-4} to 7.9×10^{-1}	1.5×10^{0} to 4.6×10^{0}			3.2×10^{5} to 1.02×10^{7}
Michel & Jolicoeur (1986)	Lab	FWI	5.0×10^{-2} to 1.0×10^{0}	2.0×10^{-2} to 9.0×10^{-2}	1.5×10^{-3} to 8.0×10^{-3}	1.7×10^{-2} to 4.0×10^{-1}	2.9×10^{-3} to 1.6×10^{-1}	1.6×10^{-3} to 8.6×10^{-3}	5.6×10^{-1} to 5.0×10^{1}			5.0×10^{5} to 1.6×10^{7}
Michel & Blanchet (1983)	Lab	FWI	5.0×10^{-2} to 1.0×10^{0}	1.2×10^{-2} to 9.0×10^{-2}	6.6×10^{-2} to 6.8×10^{-2}	7.3×10^{-1} to 5.7×10^{0}	6.7×10^{-2} to 1.4×10^{0}	7.0×10^{-2} to 2.0×10^{-1}	5.1×10^{-1} to 8.3×10^{1}	8.0×10^{9}		1.5×10^{6} to 6.5×10^{6}
Frederking & Gold (1975)	Lab	FWI	1.3×10^{-2} to 1.5×10^{-1}	2.5×10^{-2} to 9.8×10^{-2}	8.3×10^{-8} to 3.3×10^{-7}	8.7×10^{-7} to 6.6×10^{-6}	5.6×10^{-7} to 6.4×10^{-6}	8.5×10^{-8} to 4.7×10^{-7}	2.1×10^{-1} to 3.0×10^{0}	* 3.0×10^{9}	* 1.3×10^{6} (Bend)	1.7×10^{6} to 4.6×10^{6}
Kry et al (1978)	Field	FWI (Lake)	1.3×10^{-1} to 2.54×10^{-1}	1.2×10^{-2} to 5.1×10^{-2}	1.3×10^{-5} to 2.5×10^{-3}	2.5×10^{-4} to 5.1×10^{-2}	1.0×10^{-4} to 2.1×10^{-2}	1.8×10^{-5} to 7.2×10^{-3}	2.6×10^{0} to 1.1×10^{1}			6.6×10^{6} to 2.2×10^{7}
Zabilansky et al (1975)	Lab	FWI	3.8×10^{-2} to 9.1×10^{-1}	3.0×10^{-2} to 1.1×10^{-1}	6.0×10^{-4} to 5.0×10^{-1}	2.2×10^{-2} to 9.2×10^{0}	6.6×10^{-4} to 5.0×10^{0}	9.8×10^{-4} to 8.1×10^{-1}	3.7×10^{-1} to 2.9×10^{1}			3.5×10^{5} to 1.4×10^{7}
Timco (1986)	Lab	FWI	2.5×10^{-2} to 1.3×10^{-1}	6.0×10^{-3} to 3.3×10^{-2}	1.0×10^{-3} to 6.0×10^{-1}	1.2×10^{-1} to 6.5×10^{1}	3.9×10^{-2} to 6.3×10^{0}	3.5×10^{-3} to 1.7×10^{0}	5.0×10^{-1} to 2.3×10^{1}			8.0×10^{5} to 1.4×10^{7}
Inoue & Koma (1985)	Field	SWI	4.0×10^{-1} to 8.0×10^{-1}	1.1×10^{-1} to 4.3×10^{-1}	7.4×10^{-4} to 7.3×10^{-3}	1.9×10^{-3} to 2.6×10^{-2}	1.6×10^{-3} to 9.2×10^{-3}	3.8×10^{-4} to 3.8×10^{-3}	9.0×10^{-1} to 7.3×10^{0}			5.6×10^{5} to 2.0×10^{6}
Nevel et al (1977)	Lab	SWI	3.8×10^{-2} to 9.2×10^{-1}	6.6×10^{-2} to 2.2×10^{-1}	1.8×10^{-3} to 5.0×10^{-1}	1.9×10^{-2} to 5.2×10^{0}	1.8×10^{-2} to 4.2×10^{0}	2.2×10^{-3} to 5.0×10^{-1}	3.1×10^{-1} to 7.2×10^{0}		6.0×10^{4} (Bend)	7.4×10^{5} to 3.0×10^{6}
Frederking et al (1982)	Lab	SWI	5.0×10^{-2} to 5.0×10^{-1}	4.1×10^{-2} to 4.6×10^{-2}	1.0×10^{-3} to 9.0×10^{-1}	2.4×10^{-2} to 1.7×10^{1}	1.3×10^{-2} to 1.8×10^{1}	1.6×10^{-3} to 1.4×10^{0}	1.2×10^{0} to 1.1×10^{1}	* 6.0×10^{7}	* 6.0×10^{4} (Bend)	1.9×10^{5} to 3.6×10^{5}
Afanasev et al (1971)	Lab	SWI	6.0×10^{-2} to 1.8×10^{-1}	2.5×10^{-2} to 3.4×10^{-2}	1.0×10^{-2}	2.9×10^{-1} to 4.0×10^{-1}	5.5×10^{-2} to 1.7×10^{-1}	1.7×10^{-2} to 2.0×10^{-2}	1.7×10^{0} to 7.2×10^{0}		3.1×10^{4} (Bend)	1.4×10^{5} to 3.3×10^{5}
Takeuchi et al (2000)	Field	SWI	6.0×10^{-1}	3.0×10^{-2} to 3.7×10^{-1}	3.0×10^{-4} to 3.0×10^{-2}	6.7×10^{-4} to 8.0×10^{-2}	3.3×10^{-4} to 5.0×10^{-2}	1.2×10^{-4} to 1.6×10^{-2}	1.6×10^{0} to 1.5×10^{1}		1.8×10^{4} (Comp)	6.2×10^{5} to 1.7×10^{7}
Akagawa et al (2001)	Field	SWI	6.0×10^{-1} to 6.0×10^{0}	1.2×10^{-1} to 3.7×10^{-1}	3.0×10^{-4} to 3.0×10^{-2}	5.0×10^{-4} to 5.0×10^{-2}	8.0×10^{-4} to 8.0×10^{-2}	1.6×10^{-4} to 1.6×10^{-2}	1.6×10^{0} to 4.5×10^{1}			3.5×10^{5} to 3.3×10^{6}

* Personal communication to author by Dr. RMW Frederking, (November 3, 2006)

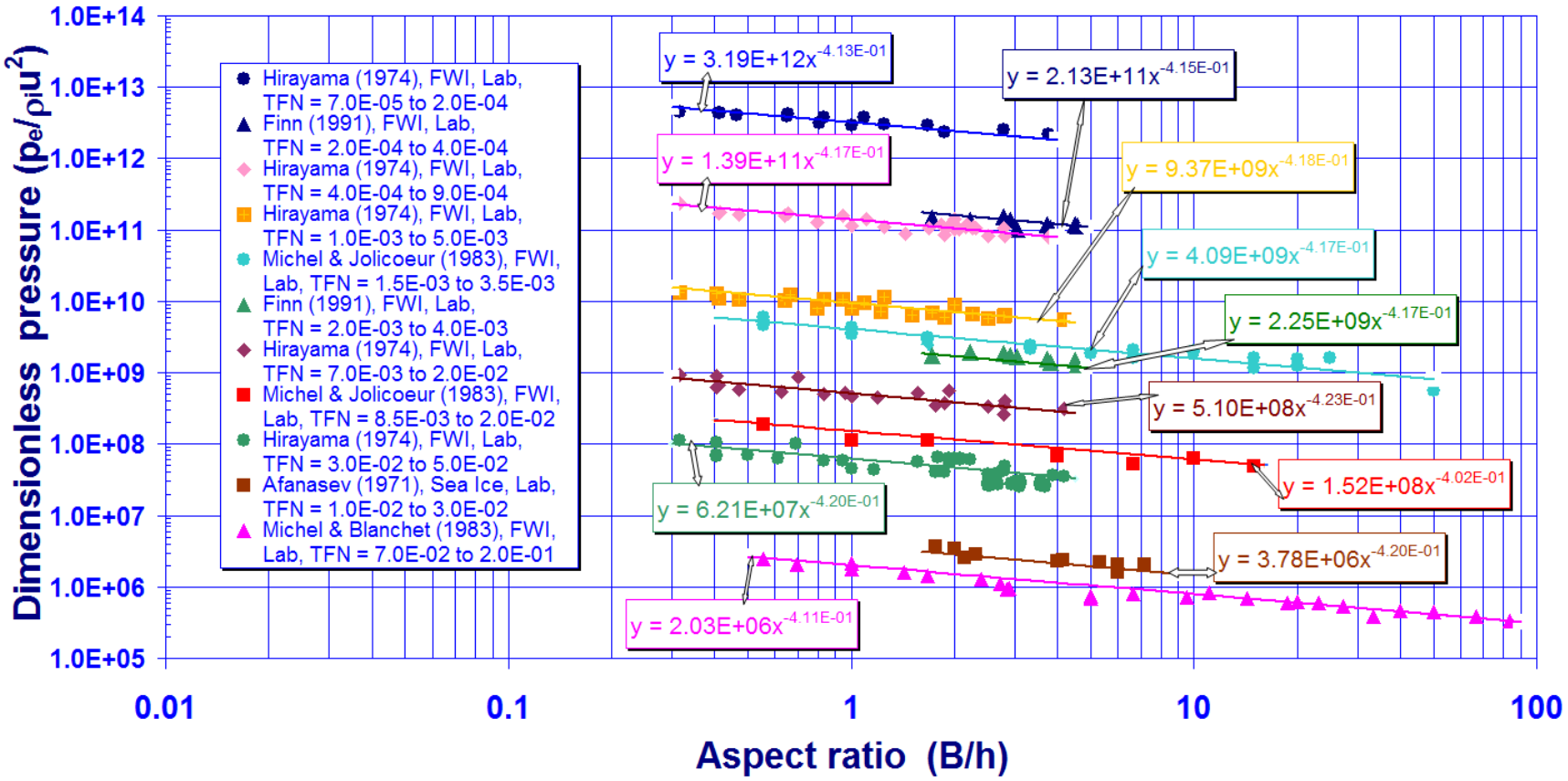

Figure 1: Dimensionless ice-induced pressure ($p_e/\rho_i u^2$) in terms of aspect ratio (B/h), for constant dimensionless velocities ($u/\sqrt{gh}$), (Freshwater Ice, Lab Tests, Data of Hirayama, 1974; Michel & Jolicoeur, 1986; Michel & Blanchet, 1983; Finn, 1991; Afanasev et al , 1971).

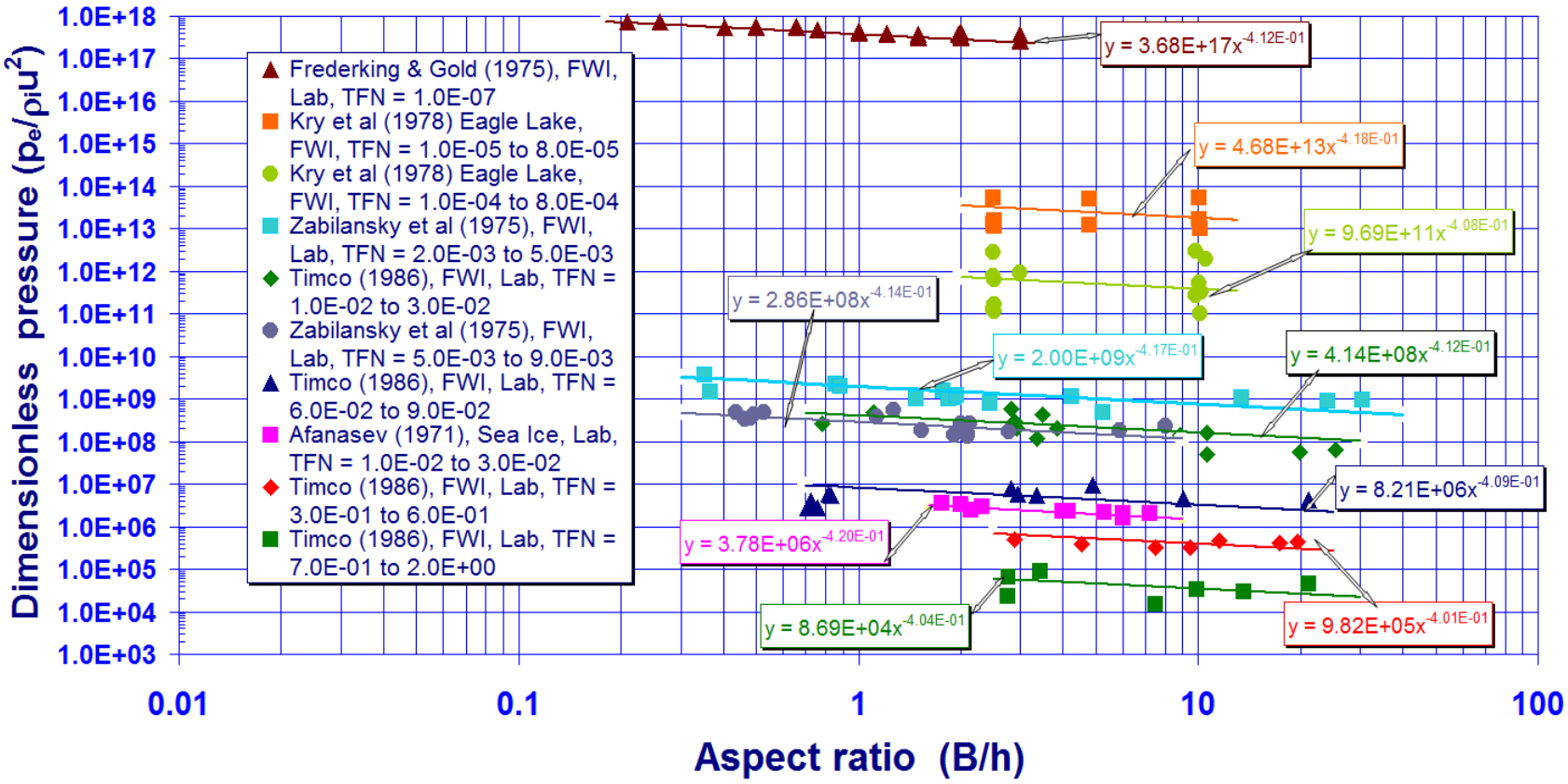

Figure 2: Dimensionless ice-induced pressure ($p_e/\rho_i u^2$) in terms of aspect ratio (B/h), for constant dimensionless velocities ($u/\sqrt{gh}$), (Freshwater Ice, Lab and Field Tests, Data of Frederking & Gold, 1975; Kry et al, 1978; Zabilansky et al, 1975; Timco, 1986; Afanasev et al, 1971).

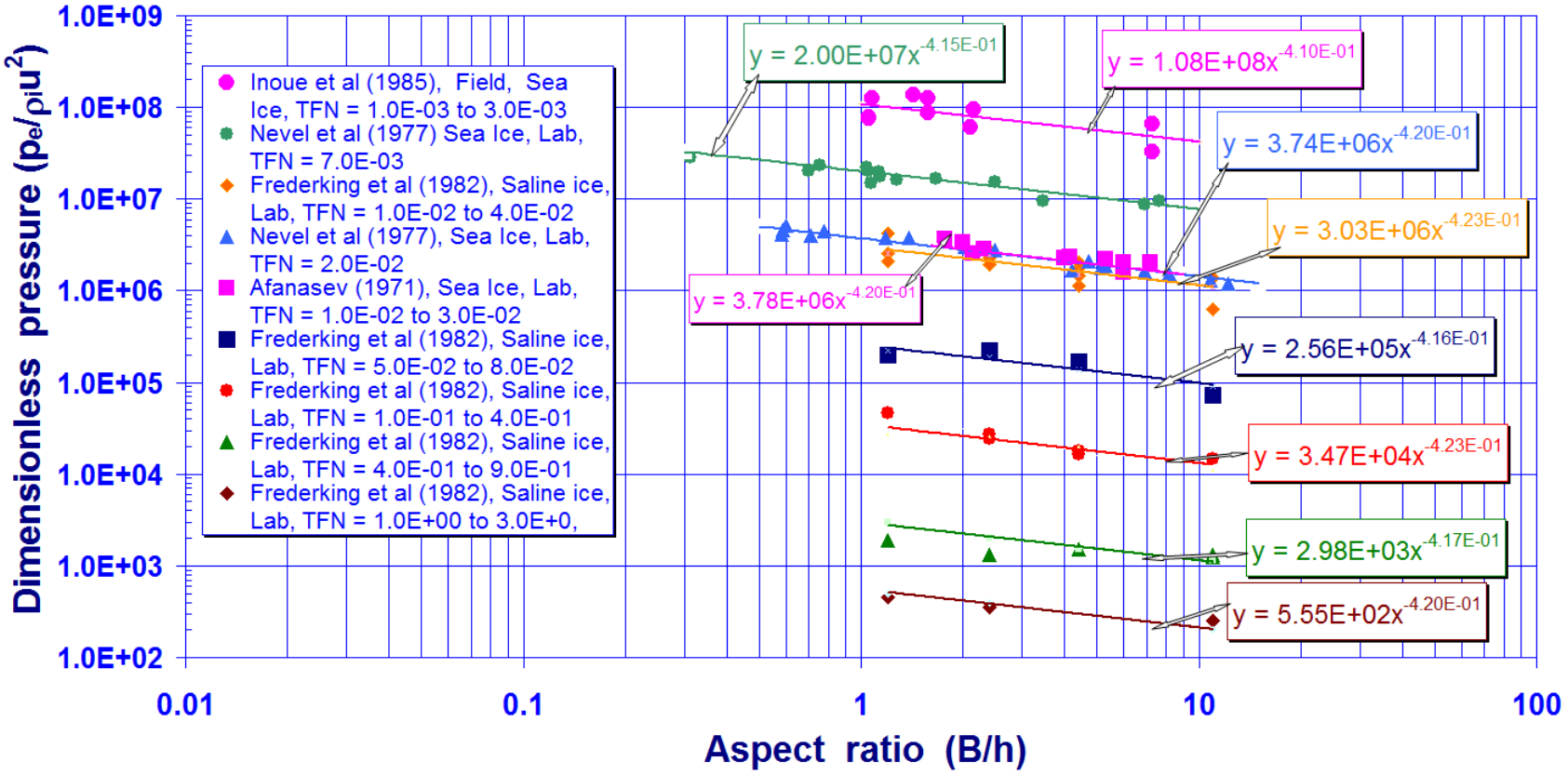

Figure 3: Dimensionless ice-induced pressure ($p_e/\rho_i u^2$) in terms of aspect ratio (B/h), for almost constant dimensionless velocities ($u/\sqrt{gh}$), (Saline ice, Field and Lab Tests of Afanasev et al, 1971; Frederking et al, 1982; Nevel et al 1977; Inoue et al, 1985).

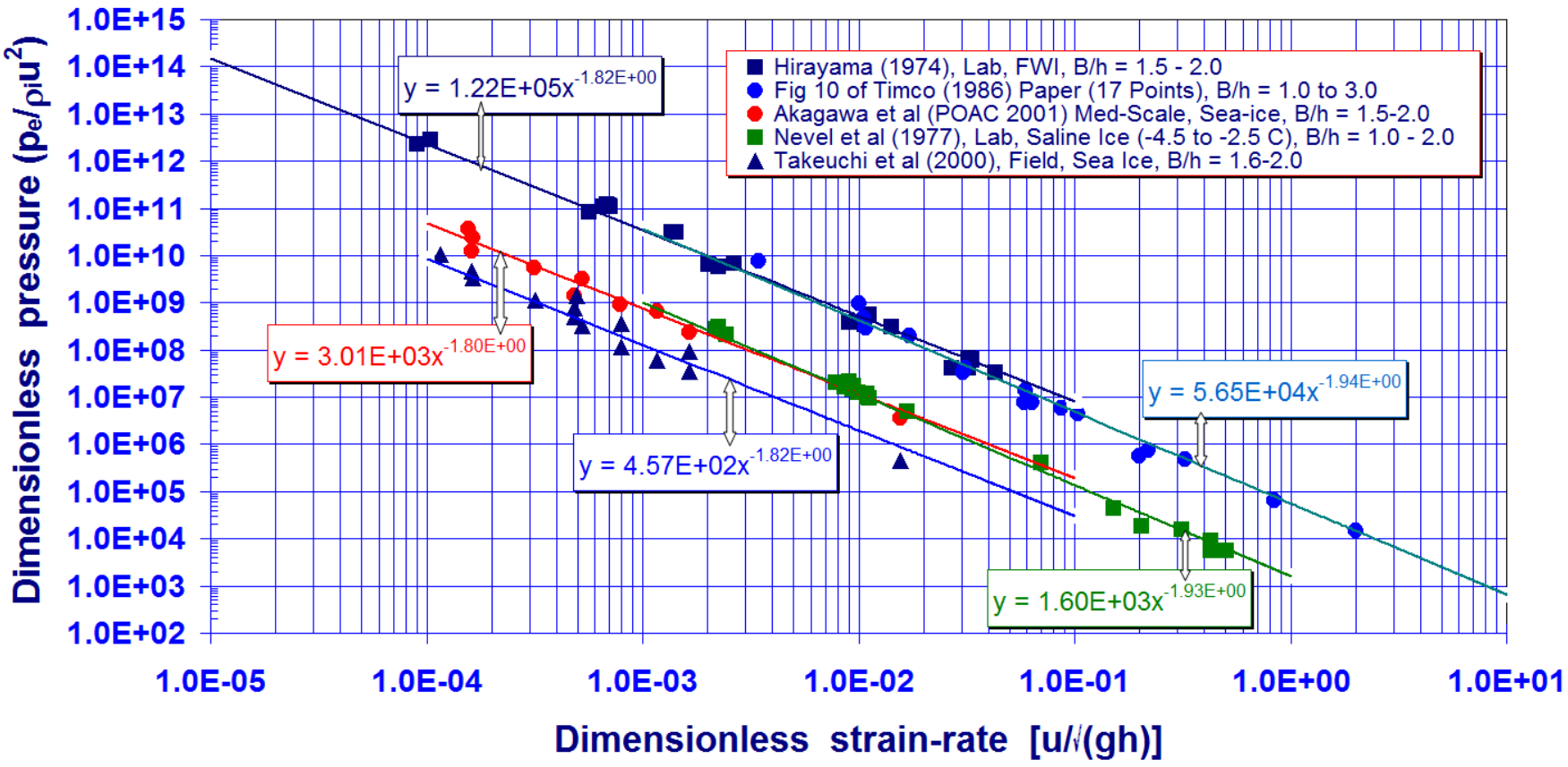

Figure 4: Dimensionless ice-induced pressure ($p_e/\rho_i u^2$) in terms of dimensionless strain-rate ($u/\sqrt{gh}$), for almost constant aspect ratio (B/h) of between 1.0 and 2.0, showing two possible slopes – milder slope for lower dimensionless strain-rate and steeper slope for higher dimensionless strain-arte (Saline ice, Field and Lab Tests of Hirayama, 1974; Timco, 1986; Nevel et al 1977; Takeuchi et al (2000); Akagawa et al, 2001).

Dimensionless ice-induced pressure ($p_e/\rho_i u^2$) as a function of aspect ratio (B/h)

In Figure 1, laboratory experimental data of Hirayama (1974), Finn (1991), Michel and Jolicoeur (1986), Michel and Blanchet (1983), are given where dimensionless ice-induced pressure ($p_e/\rho_i u^2$) is plotted as a function of aspect ratio (B/h). These data are for freshwater ice for which strain-rate (u/h) varies from about $1.0\times10^{-3}s^{-1}$ to 6.0×10^{0} s^{-1} which can be considered to be in transition from ductile deformation to brittle failure regime of ice. The corresponding dimensionless strain-rate or dimensionless velocity or thickness Froude number [$u/\sqrt{(gh)}$] for these datasets varies from about 7.0×10^{-5} to 2.0×10^{-1}.

We can see from Figure 1 two salient points: (1) that when the dimensionless velocity $u/\sqrt{(gh)}$ remains almost constant, the dimensionless ice-induced pressure ($p_e/\rho_i u^2$) of these data decreases with increasing aspect ratio (B/h) at a rate of about 0.42; (2) that at any constant aspect ratio (B/h), the data of Hirayama (1974), Finn (1991), Michel and Jolicoeur (1986), Michel and Blanchet (1983), shows that dimensionless ice-induced pressure, in general, decreases with increasing dimensionless velocity $u/\sqrt{(gh)}$. The exact quantitative nature of variation of $p_e/\rho_i u^2$ with $u/\sqrt{(gh)}$ needs to be ascertained through separate plots. We can also see that for a constant B/h, for some of the data of Hirayama, Michel and Jolicoeur, Finn, when $u/\sqrt{(gh)}$ is almost equal, for example, when $u/\sqrt{(gh)}$ is about 1.0×10^{-3} to 4.0×10^{-3} for Hirayama, Michel and Jolicoeur, Finn data, this decrease in ice induced pressure with increasing $u/\sqrt{(gh)}$ is not well defined as for others. This may be due to differences in material properties of ice used at slightly different temperatures by different researchers.

In Figure 2, laboratory experimental data of Frederking and Gold (1974), Zabilanski et al (1974) and Timco (1986) for freshwater ice and field test data of Kry et al (1978) from Eagle lake tests are plotted showing dimensionless ice-induced pressure ($p_e/\rho_i u^2$) as a function of aspect ratio (B/h). The strain-rate (u/h) for these data varies from about $8.7\times10^{-7}s^{-1}$ to 7.0×10^{1} s^{-1} which can be considered to include many forms of forms of deformation from creep to brittle failure of ice. The corresponding dimensionless strain-rate [$u/\sqrt{(gh)}$] varies from about 8.5×10^{-8} to 2.0×10^{0}. All these datasets in Figure 2 show similar variation of dimensionless ice-induced pressure as a function of B/h and $u/\sqrt{(gh)}$ as discussed in the context of Figure 1. That is, dimensionless ice-induced pressure ($p_e/\rho_i u^2$) of these data decreases with increasing aspect ratio (B/h) at a rate of about 0.42; and, at any constant aspect ratio (B/h), dimensionless ice-induced pressure, in general, decreases with increasing dimensionless velocity $u/\sqrt{(gh)}$.

In Figures 1 and 2, the data of Afanasev et al (1971) is also included. We initially harvested this data from Neill (1976). Since the original Russian report of Afanasev et al was published in the mid 1960s, we thought that this data belonged to freshwater ice and so included their data along with other freshwater ice data! However, after analyzing the data and looking at the plots shown in Figures 1 and 2 carefully, we realized that Affanasev data cannot be for freshwater ice! The reason is that at constant B/h, while all other datasets in Figures 1 and 2, in general, showed gradual decrease in dimensionless ice-induced pressure with increase in dimensionless strain-rate, the data of Afanasev et al did not have a $u/\sqrt{(gh)}$ value that followed this decreasing pattern compared to its neighbouring datasets, both in Figures 1 and 2. The question arose as to the causes of this apparent discrepancy. What is the cause for the dataset of Afanasev et al not following the patterns observed for other freshwater ice datasets? Is the material properties of Afanasev et al data substantially different from that used for freshwater ice data? Or, is the analyses performed thus far incorrect? When we looked at the original translation of Afanesev et al (1971), we found that in fact

seawater-ice was used in the laboratory experiments of a Afanesev et al (1971) and that the bending strength of ice (σ_f) used in the experiments was reported to be about 3.0×10^4Pa.

In Figure 3, field test data of Inoue et al (1971) using sea-ice and laboratory experimental data of Nevel et al (1975), Frederking et al (1982), and Afanasev et al (1971) all using sea-ice are plotted showing dimensionless ice-induced pressure ($p_e/\rho_i u^2$) as a function of aspect ratio (B/h). The strain-rate (u/h) for these data varies from about 1.0×10^{-3}s^{-1} to 2.0×10^{1} s^{-1} and the corresponding dimensionless strain-rate or thickness Froude number $u/\sqrt{(gh)}$ varies from about 4.0×10^{-4} to 1.4×10^{0}. As discussed in the context of Figures 1 and 2, all these datasets in Fig. 3, show that when $u/\sqrt{(gh)}$ is almost constant, $p_e/\rho_i u^2$ of these data decreases with increasing aspect ratio (B/h) at a rate of about 0.42; and, at any constant aspect ratio (B/h), dimensionless ice-induced pressure, in general, decreases with increasing dimensionless velocity $u/\sqrt{(gh)}$. In this figure, by including only seawater-ice data, we can see that Affanasev et al data also clearly follows the trend of decreasing dimensionless pressure with increasing $u/\sqrt{(gh)}$!

In addition, we can also see from Figure 3 that the data of Nevel et al with the symbol (▲), Frederking et al with the symbol (♦) and Afanasev et al (1971) with the symbol (■), all have dimensionless strain-rate or thickness Froude number $u/\sqrt{(gh)}$ value of about 2.0×10^{-2}. These three datasets having an almost constant value of $u/\sqrt{(gh)}$ show almost a coinciding plot, through all the aspect ratios for which data is available. What is this phenomenon due to? The explanation is this: For an almost constant value of $u/\sqrt{(gh)}$, Eqns. 2 and 3, will be reduced to:

$$\left(\frac{p_e}{\rho u^2}\right) = \phi_4\left\{\left(\frac{B}{h}\right), \left(\frac{E}{\sigma_f}\right), \left(\frac{\rho u^2}{E}\right)\right\} \qquad (2a)$$

$$\left(\frac{p_e}{\rho u^2}\right) = \phi_5\left\{\left(\frac{B}{h}\right), \left(\frac{\sigma_f\sqrt{h}}{K_{IC}}\right), \left(\frac{\rho u^2\sqrt{h}}{K_{IC}}\right), \left(\frac{E}{\sigma_f}\right)\right\} \qquad (3a)$$

which shows that $p_e/\rho_i u^2$ is a function of the aspect ratio and dimensionless material properties of ice, when dimensionless velocity is constant. When we look at the material properties of sea-ice used in the experiments (Table 1) of Afanasev et al, Nevel et al and Frederking et al we see that Afanasev et al data is obtained for a bending strength (σ_f) of about 3.0×10^4 Pa, while the data of Nevel et al and Frederking et al were obtained with ice having σ_f in the range of 6.0×10^4 Pa. Thus, the material properties of ice used in Afanasev et al, Nevel et al and Frederking et al experiments were almost same. If the material properties are also constant for the three datasets, Eqns. 2a and 2b will be reduced to:

$$\left(\frac{p_e}{\rho u^2}\right) = \phi_6\left(\frac{B}{h}\right) \qquad (2b)$$

$$\left(\frac{p_e}{\rho u^2}\right) = \phi_7\left(\frac{B}{h}\right) \qquad (3a)$$

That is if dimensionless velocity and material properties are constant for different experimental datasets, then, dimensionless pressure should be a function of aspect ratio only! That is what is depicted by the data of Nevel et al with the symbol (▲), Frederking et al with the symbol (♦) and Afanasev et al (1971) with the symbol (■). If dimensionless material properties, dimensionless velocity are constant, then, dimensionless ice-induced pressure at a constant B/h should be an invariant quantity. This is evident from these three curves in Fig. 3.

Dimensionless ice-induced pressure ($p_e/\rho_i u^2$) in terms of dimensionless strain-rate $u/\sqrt{(gh)}$

It was noted in the context of Figures 1 to 3 that at constant aspect ratio (B/h), dimensionless ice-induced pressure ($p_e/\rho_i u^2$) generally decreases with increasing dimensionless strain-rate $u/\sqrt{(gh)}$ when the material properties of ice remained constant. To quantify the influence of $u/\sqrt{(gh)}$ on ($p_e/\rho_i u^2$), dimensionless ice-induced pressures were plotted as a function of dimensionless strain-rate $u/\sqrt{(gh)}$ for almost constant aspect ratios.

In Figure 4, one such result is presented showing laboratory results using freshwater ice of Hirayama (1974) and Timco (1986) and field data of Akagawa et al (2001) and laboratory results of Nevel et al (1975) both using seawater ice. The aspect ratio of all the data, except that of Timco, shown in Figure 4 is almost constant – between 1.0 and 2.0. The aspect ratio of Timco's data varied between 1.0 and 3.0. The graphs of these data show that ($p_e/\rho_i u^2$) decreases with increasing $u/\sqrt{(gh)}$ at a rate of about 1.8 when $u/\sqrt{(gh)}$ is less than about 6.0×10^{-3}. When $u/\sqrt{(gh)}$ is greater than about 6.0×10^{-3}, the rate of variation is about 1.94. If we look at Michel's strain-rate *vs* pressure diagram, ductile deformation is up to about a strain-rate of 10^{-3} s^{-1} and fracture deformation is beyond 10^{-2} s^{-1}. For strain-rate between 10^{-3} s^{-1} and 10^{-2} s^{-1}, there is transition. Whether or not the value of $u/\sqrt{(gh)}$ of about 6.0×10^{-3} would indicate a point of transition from ductile to fracture deformation of ice needs to be confirmed through further on going analysis of various other datasets. But our analysis of most of the data so far indicate that the slope of $u/\sqrt{(gh)}$ *vs* $p_e/\rho_i u^2$ curve changes when $u/\sqrt{(gh)}$ is between 10^{-3} and 10^{-2}. We would like to point out that preliminary results of the variation of $p_e/\rho_i u^2$ as a function of $u/\sqrt{(gh)}$ for many different datasets have been reported in Arunachalam (2005; 2008;2010).

Influence of Material Properties on Dimensionless ice-induced pressure ($p_e/\rho_i u^2$)

It was pointed out that when B/h, and $u/\sqrt{(gh)}$ are both held constant, ($p_e/\rho_i u^2$) is a function of dimensionless material properties of ice alone (Eqns. 2a and 3a). In Figure 4, as explained before, the top curve is for is for freshwater ice from two datasets, middle curve is for seawater-ice for two datasets and the bottom curve is also for seawater ice for one dataset. This figure in addition to showing the influence of dimensionless velocity or dimensionless strain-rate, also shows that for constant B/h, and constant $u/\sqrt{(gh)}$, dimensionless ice-induced pressure is less for sea ice. The temperature and bending strength (σ_f) of freshwater ice for Hirayama data were about -6°C and about 3.0×10^6 Pa, respectively. A similar value can be assumed for the data of Timco, using freshwater ice. We know the bending strength of sea ice for Nevel at al data was about 6.0×10^4 Pa. A similar value can be assumed for Akagawa's field data with sea-ice, as well. It is seen from Figure 4 that for constant B/h and at constant $u/\sqrt{(gh)}$ dimensionless ice-induced pressure is about 1.8 order of magnitude less for sea ice when compared with corresponding condition for freshwater ice. The exact quantitative nature of influence of material properties of ice on $p_e/\rho_i u^2$ can be established only after completion of ongoing further analyses of various datasets with appropriate plots.

The field test results of Takeuchi et al (2000) using sea ice is also presented in Figure 4, which shows that dimensionless ice-induced pressure is slightly less for Takeuchi data when compared with the data of Nevel et al and Akagawa et al. Since other conditions remain almost same for these two datasets, we can assume that the material properties of Takeuchi et al would be slightly less than that for Nevel et al data. For estimating the quantitative influence of material properties effect on dimensionless ice-induced pressure, we are currently plotting $p_e/\rho_i u^2$ as a function of $\sigma_f^2\sqrt{h}/EK_{IC}$ as well as $p_e/\rho_i u^2$ as a function of $\sigma_f^2 h\,\rho_i u^2/EK_{IC}^2$, to find which form of representation will bring out the influence of material properties on dimensionless ice-induced pressure.

Influence of Shape of structures on Dimensionless ice-induced pressure ($p_e/\rho_i u^2$)

The influence of shape of structures has been studied in laboratory tests by some researchers - Afanasev et al (1971), Hirayama (1974), and Nevel et al (1977). In Figure 5 dimensionless ice-induced pressures is plotted as a function of dimensionless strain-rate for constant aspect ratios, for the data of Hirayama (1974) and Nevel et al (1977). They used flat, circular, wedge-shaped indentors. These two plots in Figure 5, show that dimensionless ice-induced pressure is not influenced by shape of structures. It should be pointed out that Afanasev et al (1971) data shown in Figure 3 are also for different shapes (flat, wedge shaped and cylindrical) of indentors and from this plot also it is seen that $p_e/\rho_i u^2$ is not influenced by structure shapes.

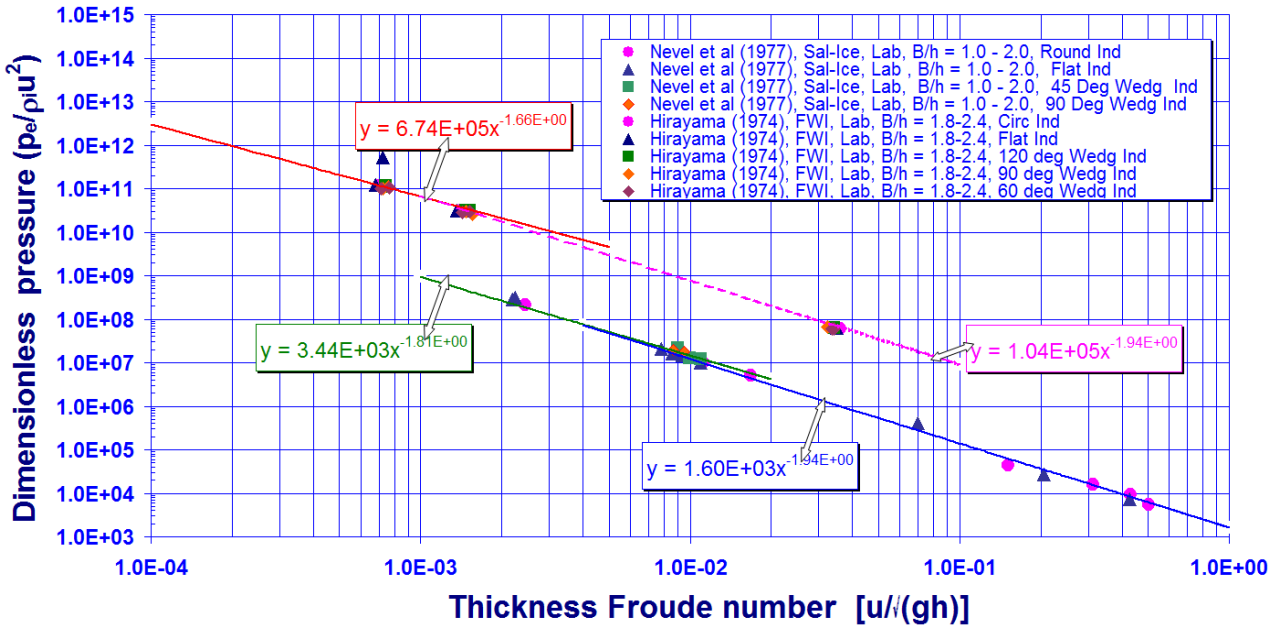

Figure 5: Dimensionless ice-induced pressure ($p_e/\rho_i u^2$) as a function of dimensionless velocities ($u/\sqrt{gh}$), *for constant aspect ratio (B/h = 1.8 to 2.4), For different shapes of structures* (Data of Hirayama, 1974, Freshwater Ice, Lab Tests; Nevel et al, 1977 , Saline Ice , Lab Tests – *Shape factor effect,*). Shapes do not seem to influence dimensionless ice-induced pressures.

The above experimental evidences and discussions indicate that analysis of experimental data in dimensionless form of variable and parameters has helped understand the physics of ice-structure interaction problem well and that for understanding ice-induced pressures on rigid vertical structures, at least 3 dimensionless parameters – aspect ratio, dimensionless velocity, dimensionless material properties have to be considered.

CONCLUSIONS

Dimensional and similitude analysis of variables defining ice-induced pressures on rigid vertical structures in conjunction with analyses of experimental data indicates that as a minimum, we should have at least three dimensionless independent parameters to define dimensionless ice-induced pressure. Analyses of a large number of experimental data from laboratory tests and field

tests, using freshwater ice, sea-ice, model-ice published by different researchers over the last 40 years, following rigorous requirements of dimensional and similitude analysis showed that (1) when other conditions remain same, dimensionless ice-induced pressures ($p_e/\rho_i u^2$) on rigid vertical structures decreases: (a) With increasing aspect ratio (B/h), at a rate of about 0.42; (b) With increasing dimensionless velocity or dimensionless strain-rate or thickness Froude number [$u/\sqrt{(gh)}$] at a rate of about 1.80 when $u/\sqrt{(gh)}$ is < about $6.0\times10^{-3}$and at a rate of about 1.93 when $u/\sqrt{(gh)}$ is > about 6.0×10^{-3}, (2) that shapes of structures do not influence dimensionless ice-induced pressures on structures. (3) When other conditions remain same, dimensionless ice-induced pressures ($p_e/\rho_i u^2$) is about 1.8 orders of magnitude less for sea-ice compared to freshwater ice. The exact quantitative influence of material property will be established when further ongoing analyses are completed.

ACKOWLEDGEMENT

The author would like to thank Dr. Mohammad Iqbal, Director, Office of Applied Research and Dr. Michael Graham, Campus Administrator, both at CNA, for their interests and encouragements in this project. Helpful comments of the anonymous reviewers are also appreciated.

REFERENCES

Afanasev, V.P., Dolgopolov, I.V., and Shvayshten, Z.I. 1971. Ice pressure on separate supporting structures in the sea, Cold Regions Research and Engrg. Laboratory (USA) Draft Translation (1971) Report no: 346, AD741873

Arunachalam, A.V.M. 2005. Application of dimensional analysis to estimation of ice-induced pressure on rigid vertical structures, Canadian Journal of Civil Engineering, Vol. **32(5)**: 968-980.

Arunachalam, A.V.M., and Graham, M.E.D., 2008. Can thickness Froude number be an influencing parameter of ice-induced pressure on vertical structures, Proc. of 9th IceTech08 Int.natl. Conf., July 2008, Paper No: ICETECH08-110-RF, Banff, Alberta, Canada.

Arunachalam, A.V.M., 2010. Combined influences of aspect-ratio, dimensionless velocity, and material properties on dimensionless ice-induced pressure on structures, Proc. of 10th IceTech10 Int.natl. Conf., Sep. 20-24, Paper No: ICETECH10-136-RF, Anchorage, Alaska, USA.

Atkins, A.G. 1975. Icebreaker modelling, Journal of Ship Research, **19(1)**: 40-43.

Atkins, A.G. 1985. Elastic and Plastic Fracture: Metals, Polymers, Ceramics, Composites, Biological Materials. Chichester, Ellis Horwood, Holsted Press.N.Y.

Barenblatt, G.I. 1996. Scaling, Self-similarity, and Intermediate Asymptotics, Cambridge University Press.

Bazant, Z.P. 1984. Size effect in blunt fracture: concrete, rock and metal, Journal of Engineering Mechanics, ASCE, vol. 110(4), paper no: 18730, pp: 518-535.

Cammaert, A.B., and Muggeridge, D.B. 1988. Ice Interaction with Offshore Structures, Van Nostrand Reinhold, N.Y.

Crawford, C.B., 1968. Ice pressures against structures, Proc. Conf. held at Laval University, Quebec, November 10-11, 1966, Associate Committee on Geotechnical Research, NRC Technical Memorandum No. 92, pp: iii.

Croasdale, K.R., and Kennedy, K.P. 1996. Ice loads consensus study update, Proc. of the 15th Int.natl. Conf. on Offshore Mechanics and Arctic Engineering, Japan Vol. 4, pp: 115-118.

Croasdale, K.R., and Brown, T.G. 2000. Ice load uncertainties - Progress in their resolution, Proc. of 10th Int.natl. Offshore and Polar Engrg. Conference, Seattle, USA, Vol. 1, pp: 583-588.

Finn, D.W. 1991. Vertical and inclined edge-indentation of freshwater ice sheets, M.Eng. Thesis, Memorial University of Newfoundland, Canada.

Frederking, R.M.W. and Gold, L.W. 1975. Experimental study of edge loading of ice plates, Canadian Geotechnical Journal, **12(4):** 456-464.

Frederking, R.M.W., Schwarz, J., Wessels, E., and Hoffman, L. 1982. Model investigations of ice forces on cylindrical structures, Proc. of Int.natl. Conf. on Marine Research, Ship Tech. and Ocean Engirg., Hamburg, Germany, pp: 341-349.

Ghoneim, G.A., Cammaert, A.B., and Mejloender-Larsen, M. 2010. Arctic challenges – A treatise of past and recent developments, Proc. of 10th IceTech10 Int.natl. Conf., Sep. 20-24, Paper No: ICETECH10-183-RF (Plenary), Anchorage, Alaska, USA.

Hirayama, K. 1974. An investigation of ice forces on vertical structures, PhD Thesis, The University of Iowa, Iowa City, USA, 153 pages.

Inoue, M.and Koma, N. 1985. Field indentation tests on cylindrical structures. Proc. of the 8th Int.natl. Conf. on Port and Ocean Engrg. under Arctic Conditions (POAC), Vol. 2, pp: 555-568, Narssarssuaq, Greenland.

Jochmann, P. and Scwarz, J. 2006. The influence of individual parameters on the effective pressure of level-ice against lighthouse Norstromsgrund, Proc. of the 18th Int.natl. Conf. Port and Oceans Engrg. under Arctic Conditions (POAC), Vol. 3, pp: 1155-1163.

Kato, K. and Sodhi, D.S. 1983. Ice action on pairs of cylindrical and conical structures, CREEL Report No: 83-25.

Korzhavin, K.N. 1971. Action of ice on engineering structures, CRREL Draft Translation Report No: TL 260, CRREL, Hanover, NH, USA, 319 pages.

Kry, P.R., Lucente, R.F., and Hedley, R.E. 1978. Continuous crushing of ice, APOA Project 106, Imperial Oil Research Department, Report No: IPRT-28ME-78., Calgary, Alberta.

Legget, R.F., and Gold, L.W., 1968. Ice pressures on structures: A Canadian problem, Proc. Conf. held at Laval University, Quebec, November 10-11, 1966, Associate Committee on Geotechnical Research, NRC Technical Memorandum No. 92, pp: 1-4.

Masterson, D.M., Frederking, R.M.W., Wright, B., Karna, T., and Maddock, W.P. 2007. A revised ice pressure-area curve, Proc. of 19th Int.natl. POAC Conference, Dalian, China, June 27-30, pp: 305-314.

Michel, B. and D. Blanchet, D. 1983. Indentation of an s_2 floating ice sheet in the brittle range, Annals of Glaciology, vol. 4, pp: 180-187.

Michel, B., and Joilicoeur, L. 1986. Experimental study of indentation of columnar-grained ice-sheet, Proc. of 5th Int.natl. Conf. on Offshore Mechanics and Arctic Engineering (OMAE), Tokyo, Vol. 4, pp: 479-488.

Michel, B., and Toussaint, N. 1977. Mechanisms and theory of indentation of ice plates. Journal of Glaciology, **19(81)**: 285-300.

Neill, C.R. 1976. Dynamic ice forces on piers and piles: An assessment of design guidelines in the light of recent research, Canadian Journal of Civil Engineering, **3(2)**: 305-341.

Nevel, D.E., Perham, R.E., and Hogue, G.B., 1977. Ice forces on vertical piles, US CRREL Report: 77-10, Hanover, NH., USA.

Palmer, A.C., Dempsey, J.P., and Masterson, D.M. 2009. A revised pressure-area curve and a fracture mechanics explanation, Cold regions science and technology, **56(2-3):** 73-76.

Sanderson, T.J.O. 1986b. Ice Mechanics: Risks to Offshore Structures, Graham and Trotman, London, UK.

Schwarz, J. 2001.Validation of low level ice forces on coastal structures, Ice in Surface waters, by HT Shen (Ed.), pp; 931 – 937.

Sharp, J.J. 1981. Hydraulic Modelling. Butterworths Publishers, Toronto.

Taylor, E.S. 1974. Dimensional analysis for engineers, Clarendon Press, Oxford, UK.

Timco, G.W. 1986. Indentation and penetration in freshwater ice. Proc.of 5th Int.natl. Conf. on Offshore Mechanics and Arctic Engineering, Tokyo, Vol. 4, pp: 444-452.

Zabilansky, L.J., Nevel, D.E., and Hynes, F.D. 1975. Ice forces on model structures, Canadian Journal of Civil Engineering, Vol. **2(4)**: 400-417.

Zufelt, J.E., and Ettema, R. 1996. Model Ice Properties. Cold Regions Research and Engrg. Laboratory, Report No: 96-1.